Simple and Efficient BZT-Higher-Order PML Formulations for the Metal Plate Buried in Three-Dimensional Dispersive Soil Space Problems

N. Feng[1], Q. H. Liu[2], and C. Zhu[1]

[1] Institute of Electromagnetics and Acoustics
Xiamen University, Xiamen, 361005, P. R. China
fengnaixing@gmail.com, zhuchhxd@xmu.edu.cn

[2] Department of Electrical and Computer Engineering
Duke University, Durham, NC 27708, USA
qhliu@ee.duke.edu

Abstract–Efficient and unsplit-field higher-order PML formulations using the stretched coordinate perfectly matched layer (SC-PML) formulations and the bilinear Z-Transform (BZT) method are presented for truncating the finite-difference time-domain (FDTD) lattices. This method is completely independent of the material properties of the FDTD computational domain and hence can be applied to the modeling of arbitrary media without any modification because of the D-B constitutive relations used. The higher-order PML has the advantages of both the conventional PML and the complex frequency-shifted PML (CFS-PML) in terms of absorbing performances. Two 3D FDTD simulations of the metal plate buried in dispersive soil space FDTD domains have been carried out to validate these formulations. It is shown that the proposed PML formulations with the higher-order scheme are efficient in terms of attenuating both the low- frequency propagating waves and evanescent waves and reducing late-time reflections.

Index Terms–Bilinear Z-transform (BZT) method, finite-difference time-domain (FDTD), and perfectly matched layer (PML).

I. INTRODUCTION

Since the introduction of the perfectly matched layer (PML) absorbing boundary condition by Berenger [1], various modified PMLs have been presented to terminate the finite-difference time-domain (FDTD) lattices. Among the various implementations of PMLs, the stretched coordinate PML (SC–PML) by Chew and Weedon [2] has the advantage of simple implementation in the corners and edges of PML regions. Furthermore, Ramadan applied Z-transform to implement PML [3]. Recently, complex frequency-shifted PML (CFS–PML), introduced by Kuzuoglu and Mittra [4] and implemented by simply shifting the frequency- dependent pole off the real axis and into the negative-imaginary half of the complex plane, has drawn considerable attention due to the fact that this PML is efficient in attenuating low-frequency evanescent waves and reducing late-time reflections [5]. However, the CFS-PML would have a poor absorption of low-frequency propagating waves as shown in [6-8]. To overcome the limitations of both the conventional PML and the CFS-PML, the higher-order PML was proposed by Correia, which retains the advantages of both the CFS-PML and conventional PML in [8]. It has shown that the 2nd-order PML is highly effective in absorbing both evanescent and low-frequency propagating waves in both open-region and periodic problems in [9]. In [9], the 2nd-order PML based on the SC-PML was implemented by using the split-field PML formulations and the auxiliary differential equation (ADE) method. However, besides the drawback of more requirements of the memory and the computational time, the

Submitted On: May 29, 2012
Accepted On: Nov. 12, 2013

higher-order PML implementation proposed in [9] was difficult to be extended to the case with more than two poles because the polynomial expansion was employed.

In this paper, efficient and unsplit-field higher-order PML formulations are proposed based on the SC-PML formulations and the bilinear Z-transform method. The proposed BZT PML algorithm is different from the proposed PML algorithm in [9] and [12-19], the proposed BZT PML algorithm is based on D-B formulations, and consequently, the proposed higher-order PML formulations require less memory and computational time as compared with that in [9]. Two 3D numerical simulation for the metal plate buried in dispersive soil space FDTD domains are given to validate the proposed formulations, as the investigation on the performance of the higher-order PML for dispersive soil half-space problem is very rare in the literatures. Only the 2nd-order case is described in this paper, but this approach is easy to be applied to any number of poles.

II. FORMULATION

In the SC-PML regions, the *x*-projection of Ampere's law for the frequency-domain modified Maxwell's equations can be written as,

$$j\omega\varepsilon_0\varepsilon_r E_x = \frac{1}{S_y}\frac{\partial H_z}{\partial y} - \frac{1}{S_z}\frac{\partial H_y}{\partial z}. \tag{1}$$

To make the PML completely independent of the material properties of the FDTD computational domain, equation (1) can be written in terms of the electric flux density D as,

$$j\omega\varepsilon_0 D_x = \frac{1}{S_y}\frac{\partial H_z}{\partial y} - \frac{1}{S_z}\frac{\partial H_y}{\partial z} \tag{2}$$

where $D_x = \varepsilon_r E_x$, ε_r is the relative permittivity of the FDTD computational domain. Consequently, this PML can be applied to truncate arbitrary media and all that is needed is to modify $D_x = \varepsilon_r E_x$ under consideration. The method is available in [11] to obtain E from D. S_η $(\eta = y, \text{or } z)$ is the complex stretched coordinate variable.

For the conventional PML, S_η is defined as,

$$S_\eta = \kappa_\eta + \sigma_\eta / j\omega\varepsilon_0 \tag{3}$$

where $\sigma_\eta \geq 0$ is the conductivity profile different from zero only in the PML region to provide attenuation for the propagating waves and $\kappa_\eta \geq 1$ is different from 1 only in the PML region to attenuate the evanescent waves.

With the CFS scheme, S_η is defined as,

$$S_\eta = \kappa_\eta + \sigma_\eta / (\alpha_\eta + j\omega\varepsilon_0) \tag{4}$$

where α_η is assumed to be positive real.

The idea of the higher-order PML was proposed in [9] by generalizing this metric for the case where more than one pole was present. For the 2nd-order PML, S_η is defined as,

$$S_\eta = S_{1\eta}\cdot S_{2\eta} = \left(\kappa_{1\eta} + \frac{\sigma_{1\eta}}{\alpha_{1\eta} + j\omega\varepsilon_0}\right) \cdot \left(\kappa_{2\eta} + \frac{\sigma_{2\eta}}{\alpha_{2\eta} + j\omega\varepsilon_0}\right). \tag{5}$$

Transforming equation (2) from the frequency domain to the *Z*-domain, we obtain,

$$\frac{1-z^{-1}}{\Delta t}\varepsilon_0 D_x = S_y(z)\cdot\frac{\partial H_z}{\partial y} - S_z(z)\cdot\frac{\partial H_y}{\partial z} \tag{6}$$

where Δt is the time step and $S_\eta(z), (\eta = y, z)$, is the *Z*-transform of $1/S_\eta$, which can be obtained by first transforming $1/S_\eta$ to the s-domain using the relation $j\omega \to s$, and then applying the bilinear transform method [10] using the relation $s \to (2/\Delta t)(1-z^{-1})/(1+z^{-1})$,

$$S_\eta(z) = w_{1\eta}\left(\frac{1-a_{1\eta}\cdot z^{-1}}{1-b_{1\eta}\cdot z^{-1}}\right)\cdot w_{2\eta}\left(\frac{1-a_{2\eta}\cdot z^{-1}}{1-b_{2\eta}\cdot z^{-1}}\right) \tag{7}$$

where

$$w_{m\eta} = \frac{2\varepsilon_0 + \alpha_{m\eta}\Delta t}{2\varepsilon_0\kappa_{m\eta} + \alpha_{m\eta}\kappa_{m\eta}\Delta t + \sigma_{m\eta}\Delta t}, \quad m=1,2$$

$$a_{m\eta} = \frac{2\varepsilon_0 - \alpha_{m\eta}\Delta t}{2\varepsilon_0 + \alpha_{m\eta}\Delta t}, \quad m=1,2,$$

$$b_{m\eta} = \frac{2\varepsilon_0\kappa_{m\eta} - \alpha_{m\eta}\kappa_{m\eta}\Delta t + \sigma_{m\eta}\Delta t}{2\varepsilon_0\kappa_{m\eta} + \alpha_{m\eta}\kappa_{m\eta}\Delta t + \sigma_{m\eta}\Delta t}, \quad m=1,2.$$

Substituting equation (7) into equation (6), we obtain,

$$\frac{1-z^{-1}}{\Delta t}\varepsilon_0 D_x = w_{1y}\left(\frac{1-a_{1y}\cdot z^{-1}}{1-b_{1y}\cdot z^{-1}}\right)\cdot w_{2y}\left(\frac{1-a_{2y}\cdot z^{-1}}{1-b_{2y}\cdot z^{-1}}\right)\cdot\frac{\partial H_z}{\partial y} - w_{1z}\left(\frac{1-a_{1z}\cdot z^{-1}}{1-b_{1z}\cdot z^{-1}}\right)\cdot w_{2z}\left(\frac{1-a_{2z}\cdot z^{-1}}{1-b_{2z}\cdot z^{-1}}\right)\cdot\frac{\partial H_y}{\partial z}. \tag{8}$$

Introducing four auxiliary variables $Q_{x\eta}$ and $P_{x\eta}$ $(\eta = y, z)$,

$$Q_{xy} = \frac{w_{1y} w_{2y} \Delta t}{\varepsilon_0} \cdot \left(\frac{1}{1 - b_{1y} \cdot z^{-1}} \right) \cdot \frac{\partial H_z}{\partial y} = b_{1y} \cdot z^{-1} Q_{xy} + \frac{w_{1y} w_{2y} \Delta t}{\varepsilon_0} \cdot \frac{\partial H_z}{\partial y} \quad (9)$$

$$P_{xy} = \left(\frac{1 - a_{2y} \cdot z^{-1}}{1 - b_{2y} \cdot z^{-1}} \right) Q_{xy} = b_{2y} \cdot z^{-1} P_{xy} + Q_{xy} - a_{2y} \cdot z^{-1} Q_{xy} \ , \quad (10)$$

$$Q_{xz} = \frac{w_{1z} w_{2z} \Delta t}{\varepsilon_0} \cdot \left(\frac{1}{1 - b_{1z} \cdot z^{-1}} \right) \cdot \frac{\partial H_y}{\partial z} = b_{1z} \cdot z^{-1} Q_{xz} + \frac{w_{1z} w_{2z} \Delta t}{\varepsilon_0} \cdot \frac{\partial H_y}{\partial z} \ , \quad (11)$$

$$P_{xz} = \left(\frac{1 - a_{2z} \cdot z^{-1}}{1 - b_{2z} \cdot z^{-1}} \right) Q_{xz} = b_{2z} \cdot z^{-1} P_{xz} + Q_{xz} - a_{2z} \cdot z^{-1} Q_{xz} \ . \quad (12)$$

Considering that the z^{-1} operator corresponds to a single-step delay in the discrete time domain, equation (9) to equation (12) can be written in the FDTD form, respectively, as equation (13) to equation (16), where

$$Q_{xy}\Big|_{i+1/2,j,k}^{n+1} = b_{1y(j)} \cdot Q_{xy}\Big|_{i+1/2,j,k}^{n} + u_{y(j)} \cdot \left(H_z\Big|_{i+1/2,j+1/2,k}^{n+1/2} - H_z\Big|_{i+1/2,j-1/2,k}^{n+1/2} \right), \quad (13)$$

$$P_{xy}\Big|_{i+1/2,j,k}^{n+1} = b_{2y(j)} \cdot P_{xy}\Big|_{i+1/2,j,k}^{n} + Q_{xy}\Big|_{i+1/2,j,k}^{n+1} - a_{2y(j)} \cdot Q_{xy}\Big|_{i+1/2,j,k}^{n}, \quad (14)$$

$$Q_{xz}\Big|_{i+1/2,j,k}^{n+1} = b_{1z(k)} \cdot Q_{xz}\Big|_{i+1/2,j,k}^{n} + u_{z(k)} \cdot \left(H_y\Big|_{i+1/2,j,k+1/2}^{n+1/2} - H_y\Big|_{i+1/2,j,k-1/2}^{n+1/2} \right), \quad (15)$$

$$P_{xz}\Big|_{i+1/2,j,k}^{n+1} = b_{2z(k)} \cdot P_{xz}\Big|_{i+1/2,j,k}^{n} + Q_{xz}\Big|_{i+1/2,j,k}^{n+1} - a_{2z(k)} \cdot Q_{xz}\Big|_{i+1/2,j,k}^{n} \ . \quad (16)$$

Equation (8) can be written as,

$$D_x\Big|_{i+1/2,j,k}^{n+1} = D_x\Big|_{i+1/2,j,k}^{n} + P_{xy}\Big|_{i+1/2,j,k}^{n+1} - a_{1y(j)} \cdot P_{xy}\Big|_{i+1/2,j,k}^{n} - \left(P_{xz}\Big|_{i+1/2,j,k}^{n+1} - a_{1z(k)} \cdot P_{xz}\Big|_{i+1/2,j,k}^{n} \right) \quad (17)$$

where $u_y = w_{1y} w_{2y} \Delta t / \varepsilon_0 \Delta y$ and $u_z = w_{1z} w_{2z} \Delta t / \varepsilon_0 \Delta z$. Δy and Δz are space step. A similar method can be used for other regions of SC-PML.

In order to perform a comparison between the proposed higher-order PML formulations and the higher-order PML formulations proposed in [9] in terms of the amount of the auxiliary variables, we assume an FDTD computational domain of L × M × N cells with W-cell thick PML used on each one of the sides of domain. In the SC-PML region, the higher-order PML formulations proposed in [9] totally requires $288W^3 + 112(LW^2+MW^2+NW^2) + 40(LMW+LNW+MNW)$ auxiliary variables, however, the proposed higher-order PML formulations totally requires $192W^3 + 64(LW^2+MW^2+NW^2) + 16(LMW+LNW+MNW)$ auxiliary variables. As a result, the proposed higher-order PML formulations save $96W^3 + 48(LW^2+MW^2+NW^2)+24(LMW+LNW+MNW)$ auxiliary variables as compared with the higher-order PML formulations proposed in [9]. Saving auxiliary variables multiply by each variable, which occupies number of bytes in memory, which can be concluded that the proposed higher-order PML formulations save memory as compared with the higher-order PML formulations proposed in [9]. Obviously, if an FDTD computational domain (L, M, and N) is constant, saving memory will increase as the increase of PML layers. Similarly, if PML layers are constant, saving memory will increase as the increase of FDTD computational domain (L, M, and N).

It is obvious that, because of no polynomial expansion, the proposed implementation of the higher-order PML is easier than that in [9] to be extended to the case with more than two poles.

III. NUMERICAL RESULT

To show the validity of the proposed formulations, we implement a 3D FDTD simulation for the metal plate buried in an inhomogeneous, dispersive, and conductive soil half-space problem in a highly elongated FDTD grid. The metal plate size is $40 \times 10 \times 2$. The dielectric constant of soil is specified as the second-order Debye model with an added conductivity term $\varepsilon_r(\omega) = \varepsilon_\infty + \sigma / j\omega\varepsilon_0 + \sum_{p=1}^{2} A_p / (1 + j\omega\tau_p)$, where $\varepsilon_\infty = 4.15$ is the infinite frequency permittivity, A_1=1.8 and A_2=0.6 are the pole amplitudes, τ_1 =3.79 nsec and τ_2=0.151 nsec are the relaxation time and σ=1.11

ms/m is the conductivity. The half-space occupies 50 % of the vertical height of the horizontally elongated simulation region. The space is discretized with the FDTD lattice with $\Delta x = \Delta y = \Delta z = 0.05$ m and time step is $\Delta t = 77$ ps. The simulation is done with a $126 \times 46 \times 26$ grid including 10-cell thick PML layers, as shown in Fig. 1. Assuming that the origin is at a corner of the FDTD grid, a vertically polarized point source located at (13, 13, 13) (above the soil) is excited by a differentiated Gaussian pulse with a half pulse bandwidth $= 1155$ ps. Within the PML, σ_η and κ_η are scaled using a fourth-order polynomial scaling and α_η is a constant. The relative reflection error (in decibels) versus time is computed at an observation point located at (113, 33, 12) using error (decibels) $R_{dB}(t) = 20\log_{10}(|E_z^R(t) - E_z^T(t)|/|E_{z\_\max}^R|)$ where $E_z^T(t)$ is the field computed using the test domain, and $E_z^R(t)$ is the reference field based on an extended lattice, and $E_{z\_\max}^R$ is the maximum value of the reference solution over the full-time simulation. For the 2nd-order PML, the relative reflection error between the formulations in [9] and the proposed formulations is first computed over 1500 time steps for $\sigma_{1\eta\text{opt}} = 0.175/150\pi\Delta x$, $\kappa_{1\eta} = 1$, $\alpha_{1\eta} = 0$, $\sigma_{1\eta} = \sigma_{1\eta\text{opt}}\rho^4$, $\alpha_{2\eta} = 0.0055 + \sigma_{1\eta}$, $\sigma_{2\eta} = \sigma_{2\eta\text{opt}}\rho^2$, $\kappa_{2\eta} = 1 + \kappa_{2\eta\text{opt}}\rho^2$, $\kappa_{2\eta\text{opt}} = 10$ and $\sigma_{2\eta\text{opt}} = 4/150\pi\Delta x$. Where the σ_{opt} is chosen as $\sigma_{\text{opt}} = (m+1)/150\pi\Delta x$ and ρ is zero at the interface of the PML and the FDTD computational domains and 1 at the end. This same example is repeated with the SC-PML ($\alpha_\eta = 0$, $\kappa_{\max} = 11$ and $\sigma_{\max} = 0.18$ S/m) and the convolution PML in [5] ($\alpha_\eta = 0.0055$, $\sigma_{\max} = 0.24$ S/m and $\kappa_{\max} = 7$). In this paper, σ and κ are evaluated as the average value in the cell around the index location [1]. These optimum parameters are chosen empirically to obtain the lowest reflection. The results are illustrated in Fig. 2.

The maximum relative reflection errors of the conventional SC-PML, the CPML, the 2nd-order PML in [9], and the proposed 2nd-order PML are -45dB, -52dB, -62dB and -70dB, respectively. It can be concluded from Fig. 2 that the absorbing performance of the proposed 2nd-order PML formulations have 18 dB and 25 dB improvement in terms of the maximum relative error as compared with the CPML and the SC-PML, respectively, and holds much lower reflection error for the late-time region than the CPML and the SC-PML. Table I and II are using different perfectly matched layer algorithm procedures, which occupy of memory and different time steps, and computational time, respectively. Obviously, when FDTD computational domain is invariant, saving memory will increase with the increase of PML layers and saving time will increase with the increase of time steps.

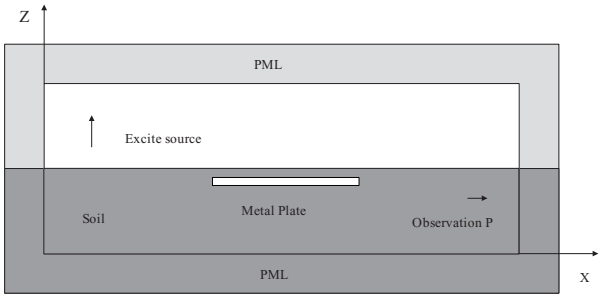

Fig. 1. A metal plate buried in an inhomogeneous, dispersive, and conductive soil half-space problem.

Table I: Memory requirements (bytes) for the different PML implementations.

	PML layers=10	PML layers=16
2nd-order PML in [9]	49,506K	105,509K
Proposed 2nd-order PML	30,848K	65,244K
CPML	24,084K	49,664K
SC-PML	24,084K	49,672K

In the second numerical example, in order to validate the proposed formulations, the problem of the electromagnetic scattering by a highly elongated object is studied. Particularly, a thin 100 mm $\times$ 25 mm plate is immersed in a background media [5] with constitutive parameters ε and σ. For the purposes of this study, constitutive parameters for soil are assumed, giving σ =0.273 and ε_r =7.73. The plate is illuminated by a vertically polarized electric current element placed just above one corner of the plate. The current source is given a differentiated Gaussian time signature with a 6 GHz bandwidth. The simulation is done with a

$126 \times 51 \times 26$ grid including 10-cell-thick PML layers placed only three cells from the scatter on all sides with the space steps $\Delta x = \Delta y = \Delta z = 5$ mm, as shown in Fig. 3. Within the PML, σ_i and κ_i are scaled using an mth order polynomial scaling. It is noted that α is not scaled, and is constant through the PML.

Table II: Computational time (s) for different PML implementations (PML layers = 10).

	Time steps =2000	Time steps =4000
2nd-order PML in [9]	757.90	1390.48
Proposed 2nd-order PML	484.18	828.30
CPML	312.48	625.08
SC-PML	314.55	626.53

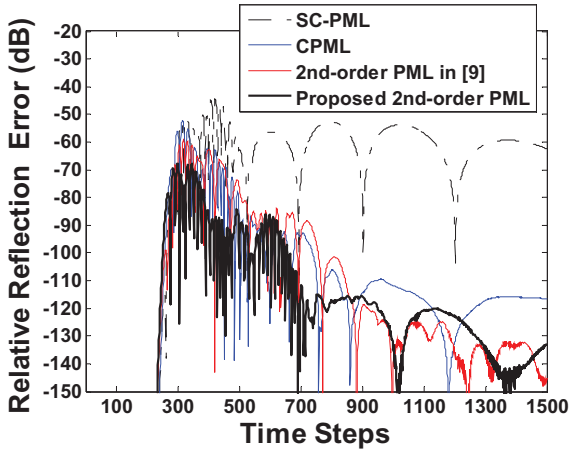

Fig. 2. The relative reflection error of the conventional SC-PML, the CPML, the 2nd-order PML in [9] and the proposed 2nd-order PML for a metal plate buried on an inhomogeneous, dispersive, and conductive soil half-space problem.

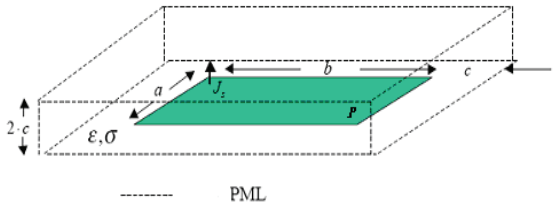

Fig. 3. Shows the FDTD grid geometry in this simulation.

To study the reflection error due to the proposed PMLs, a reference problem is also simulated. To this end, the same mesh is extended 75 cells out in all dimensions, leading to a 272 × 201 × 176 cell lattice. The proposed PMLs are used to terminate this lattice with optimal PML parameters to minimize any spurious reflection. The fields within the lattice are then excited by an identical source, and the time-dependent fields are recorded within the region representing the original lattice. The relative reflection error (in dB) versus time is computed at an observation point in the corner of the computational domain using $R_{dB}(t)=20\log_{10}\left(\left|E_x(t)-E_{\text{xref}}(t)\right|\Big/\left|E_{\text{x\_refmax}}\right|\right)$ where $E_x(t)$ represents the time-dependent discrete electric field of the observation point, $E_{\text{xref}}(t)$ is a reference solution based on an extended lattice, and $E_{\text{x\_refmax}}$ represents the maximum value of the reference solution over the full-time simulation. The relative error computed is recorded in Fig. 4. The relative reflection error is first computed over 1800 time iterations. This same example is repeated with SC-PML (α_η =0 $\kappa_{\max}$ =14 and $\sigma_{\max}$ =2.290 S/m) and the convolution PML (CPML) [5] (α_η =0.04 $\kappa_{\max}$ =11 and $\sigma_{\max}$ =4.198 S/m). For the 2nd-order PML including the proposed PML formulations and the formulations in [9], the following parameters are chosen: $\kappa_{1\eta}$ =1, $\alpha_{1\eta}=0$, $\sigma_{1\eta\text{opt}}=0.175/150\pi\Delta x$, $\sigma_{1\eta}=\sigma_{1\eta\text{opt}}\rho^4$, $\kappa_{2\eta\text{opt}}=14$, $\kappa_{2\eta}=1+\kappa_{2\eta\text{opt}}\rho^2$, $\alpha_{2\eta}=0.04+\sigma_{1\eta}$, $\sigma_{2\eta\text{opt}}=4/150\pi\Delta x$ and $\sigma_{2\eta}=\sigma_{2\eta\text{opt}}\rho^2$, where ρ is zero at the interface of the PML and the FDTD computational domains and 1 at the end. In all computations of this paper, σ and κ are evaluated as the average value in the cell around the index location [1]. These optimum parameters are chosen empirically to obtain the lowest reflection.

These results are illustrated from Fig. 4. The maximum relative reflection errors of the conventional SC-PML, the CPML, the proposed 2nd-order PML and the 2nd-order PML in [9] are -50dB, -86dB, -93dB, and -93dB, respectively. It can be concluded from Fig. 4 that the absorbing

performance of the proposed 2nd-order PML formulations has more 7dB and 43dB improvement in terms of the maximum relative error as compared with the CPML and the SC-PML, respectively, and holds much lower reflection error for the late-time region than the SC-PML.

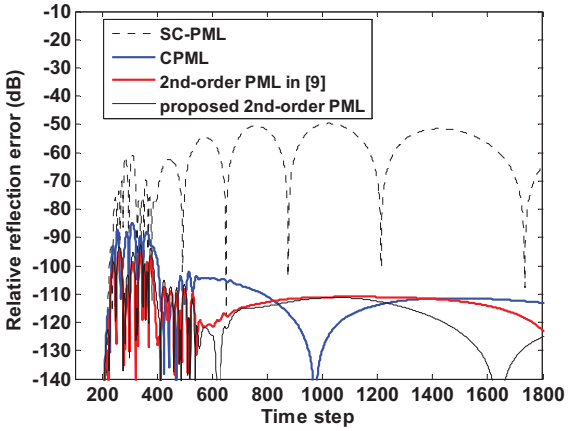

Fig. 4. The relative reflection error of the conventional SC-PML, the CPML, the 2nd-order PML in [9] and the proposed 2nd-order PML.

Tables III and IV are using different perfectly matched layer algorithm procedures, which occupy memory and different time steps, which occupy of computational time, respectively. Obviously, when FDTD computational domain is invariant, saving memory will increase with the increase of PML layers and saving time will increase with the increase of time steps.

Table III: Memory requirements (bytes) for the different PML implementations.

	PML layers=10	PML layers=16
2nd-order PML in [9]	43,803K	98,748K
Proposed 2nd-order PML	31,288K	65,832K
CPML	25,343K	53,323K
SC-PML	26,332K	55,428K

IV. CONCLUSION

Efficient and unsplit-field higher-order PML formulations based on the SC-PML and the bilinear Z-transform method has been presented. It can be shown in the numerical simulation that the proposed 2nd-order PML formulations hold good absorbing performance in terms of attenuating both the low-frequency propagating waves and evanescent waves, and also require less memory and computational time as compared with that in [9].

Table IV: Computational time (s) for the different PML implementations (PML layers=10).

	Time steps =1000	Time steps =2000
2nd-order PML in [9]	707.37	1443.65
Proposed 2nd-order PML	500.98	1031.18
CPML	378.07	777.51
SC-PML	381.70	780.51

ACKNOWLEDGMENT

This work is supported by the Natural Science Foundation of China (NSFC) under Grant 412400 29 and 61301008.

REFERENCES

[1] J. Bérenger, "A perfectly matched layer for the absorption of electromagnetic waves," *J. Computat. Phys.*, vol. 114, no. 2, pp. 185-200, Oct. 1994.

[2] W. Chew and W. Weedon, "A 3-D perfectly matched medium from modified Maxwell's equations with stretched coordinates," *Microw. Opt. Technol. Lett.*, vol. 7, no. 13, pp. 599-603, Sep. 1994.

[3] O. Ramadan and A. Oztoprak, "Z-transform implementation of the perfectly matched layer for truncating FDTD domains," *IEEE Microw. Wireless Compon. Lett.*, vol. 13, no. 9, pp. 402-404, Sep. 2003.

[4] M. Kuzuoglu and R. Mittra, "Frequency dependence of the constitutive parameters of causal perfectly matched anisotropic absorbers," *IEEE Microw. Guided Wave Lett.* , vol. 6, no. 12, pp. 447-449, Dec. 1996.

[5] J. Roden and S. Gedney, "Convolution PML (CPML): An efficient FDTD implementation of the CFS-PML for arbitrary media," *Microw. Opt. Technol. Lett.*, vol. 27, no. 5, pp. 334-339, Dec. 2000.

[6] E. Bécache, P. Petropoulus, and S. Gedney, "On the long-time behavior of unsplit perfectly matched layers," *IEEE Trans. Antennas Propag.*, vol. 52, no. 5, pp. 1335-1342, May 2004.

[7] J. Bérenger, "Numerical reflection from FDTD-PMLs: a comparison of the split PML with

the unsplit CFS PML," *IEEE Trans. Antennas Propag.*, vol. 50, no. 3, pp. 258-265, March 2002.

[8] D. Correia and J. Jin, "Performance of regular PML, CFS-PML, and second-order PML for waveguide problems," *Microw. Opt. Technol. Lett.*, vol. 48, no. 10, pp. 2121-2126, Oct. 2006.

[9] D. Correia and J. Jin, "On the development of a higher-order PML," *IEEE Trans. Antennas Propag.*, vol. 53, no. 12, pp. 4157-4163, Dec. 2005.

[10] J. Proakis and D. Manolakis, *Digital Signal Processing: Principles, Algorithms and Applications*, 3rd ed. Englewood Cliffs, NJ: Prentice Hall, 1996.

[11] D. Sullivan, "Frequency-dependent FDTD methods using Z transforms," *IEEE Trans. Antennas Propag.*, vol. 40, no. 10, pp. 1223-1230, 1992.

[12] O. Montazeri, M. Bakr, and Y. Haddara, "A PML for electroacoustic waves in piezoelectric materials using FDTD," *The Applied Computational Electromagnetics Society (ACES) Journal*, vol. 26, no. 6, pp. 464-472, June 2011.

[13] N. Okada and J. Cole, "Nonstandard finite difference time domain algorithm for Berenger's perfectly matched layer," *The Applied Computational Electromagnetics Society (ACES) Journal*, vol. 26, no. 2, pp. 153-159, Feb. 2011.

[14] J. Cole and D. Zhu, "Improved version of the second-order Mur absorbing boundary condition based on a nonstandard finite difference model," *The Applied Computational Electromagnetics Society (ACES) Journal*, vol. 24, no. 4, pp. 375-381, August 2009.

[15] M. Wong and A. Sebak, "The floating PML applied to practical FDTD applications," *The Applied Computational Electromagnetics Society (ACES) Journal*, vol. 23, no. 2, pp. 110-119, June 2008.

[16] M. Inman, A. Elsherbeni, J. Maloney, and B. Baker, "Practical implementation of a CPML absorbing boundary for GPU accelerated FDTD technique," *The Applied Computational Electromagnetics Society (ACES) Journal*, vol. 23, no. 1, pp. 16-22, March 2008.

[17] T. Kaufmann, K. Sankaran, C. Fumeaux, and R. Vahldieck, "A review of perfectly matched absorbers for the finite-volume time-domain method," *The Applied Computational Electromagnetics Society (ACES) Journal*, vol. 23, no. 3, pp. 184-192, Sep. 2008.

[18] N. Feng and J. Li, "Novel and efficient FDTD implementation of higher-order perfectly matched layer based on ADE method," *J. Computat. Phys.*, vol. 232, no. 1, pp. 318-326, Jan. 2013.

[19] G. Fan and Q. Liu, "A well-posed PML absorbing boundary condition for lossy media," *in Proc. IEEE Antennas Propagat. Soc. Int. Symp. Dig.*, vol. 3, pp. 2-5, Boston, MA, July 8–13, 2001. *It is also published in Antennas Wireless Propag. Lett.*, vol. 2, pp. 97-100, 2003.

Naixing Feng received the B.S. degree in Electronic Science and Technology and the M.S. degree in Micro- Electronics and Solid-State electronics from Tianjin Polytechnic University, Tianjin, China, in 2010 and 2013, respectively. He is currently working toward his PhD degree in Radio Physics at Xiamen University, Xiamen. His current research interests include computational electromagnetics and acoustics.

Qing Huo Liu received his B.S. and M.S. degrees in physics from Xiamen University in 1983 and 1986, and Ph.D. degree in electrical engineering from the University of Illinois at Urbana-Champaign in 1989.

His research interests include computational electromagnetics and acoustics, inverse problems, geophysical subsurface sensing, biomedical imaging, electronic packaging, and the simulation of photonic and nano devices. He has published over 500 papers in refereed journals and conference proceedings. He was with the Electromagnetics Laboratory at the University of Illinois at Urbana-Champaign as a Research Assistant from September 1986 to December 1988, and as a Postdoctoral Research Associate from January 1989 to February 1990. He was a Research Scientist and Program Leader with Schlumberger-Doll Research, Ridgefield, CT from 1990 to 1995. From 1996 to May 1999 he was an Associate Professor with New Mexico State University. Since June 1999, he has been with Duke University where he is now a Professor of Electrical and Computer Engineering.

Dr. Liu is a Fellow of the IEEE, a Fellow of the Acoustical Society of America, a member of Phi Kappa Phi, Tau Beta Pi, a full member of U.S. National Committee of URSI Commissions B and F. Currently he serves as the Deputy Editor in Chief of Progress in Electromagnetics Research, an Associate Editor for IEEE Transactions on Geoscience and Remote Sensing, and an Editor for Computational Acoustics. He was a Guest Editor in Chief of Proceedings of the IEEE for a special issue on large-scale computational electromagnetics published in 2013. He received the 1996 Presidential Early Career Award for Scientists and Engineers (PECASE) from the White House, the 1996

Early Career Research Award from the Environmental Protection Agency, and the 1997 CAREER Award from the National Science Foundation.

Chunhui Zhu received the Ph.D. degree in control science and engineering from Harbin Institute of Technology, in 2012. From October 2009 to October 2011, she was with the electrical engineering at Duke University, Durham, NC, as a visiting student. Since January 2013, she has been with Xiamen University, where she is currently an assistant professor of department of electronic science. Her research interest is fast algorithms for computational electromagnetics and their applications in engineering.